Mon. Not. R. Astron. Soc. **000**, 1–10 (1997) Printed 9 June 1997 (MN LaTeX style file v1.4)

The mass of the black hole in the low inclination LMXB transient system GRO J0422+32 (= Nova Persei 1992)

G.Beekman[1], T.Shahbaz[2], T.Naylor[1], P.A.Charles[2], R.M.Wagner[3] & P.Martini[3]

[1] *Department of Physics, Keele University, Staffordshire ST5 5BG*
[2] *Department of Astrophysics, Nuclear Physics Laboratory, Keble Road, Oxford OX1 3RH*
[3] *Department of Astronomy, Ohio State University, 174 West 18th Avenue, Columbus, OH 43210*

Accepted ???. Received ???; In original form ???.

ABSTRACT

We present the first infrared light curve of GRO J0422+32, and use it along with R-band data and published I- and Cousins R_c- band data to constrain the inclination of the system to be between 10 and 26 degrees, implying that the black hole mass is greater than $\sim$15M$_\odot$ Re-modelling the data with a 30 percent accretion disc contamination level changes the result little, the new limits being 13-31 degrees for the inclination, and greater than $\sim$9M$_\odot$ for the mass. Our results are the lowest inclination and, consequently, the highest mass claims yet made for this system. Previous observations of dips seen during outburst are suggestive of a partial eclipse. Here we show that an eclipse interpretation of the so-called orbital dips is inconsistent with other data; the "dips" are more likely to be random luminosity variations of a disc in outburst.

We also show, for the first time, how an equation by King et al. (1996) allows a lower limit to the compact object mass in the SXTs to be independently estimated by use of the orbital period and spectral type only. This allows the spectroscopist to immediately identify the strong black hole candidates amongst SXTs with orbital periods $\lesssim$ 2 days. These new mass estimates are in agreement with the ellipsoidally determined mass estimates, and indicate that GRO J0422+32 contains a black hole with a mass $\gtrsim$28M$_\odot$.

Key words: binaries: close – black hole physics – infrared: stars – stars: fundamental parameters – stars: individual: GRO J0422+32 – X-rays: stars.

1 INTRODUCTION

The soft X-ray transients (SXTs), or X-ray novae, are a subset of the low-mass X-ray binaries [LMXBs; see reviews by Bradt & McClintock (1983), van der Klis (1989), Cowley (1992), Verbunt (1993), Tanaka & Lewin (1995), van Paradijs & McClintock (1995)]. They consist of a late-type star (the secondary), a compact object (the primary), which is either a neutron star or a black hole, and an accretion disc (formed as a result of mass transfer from the secondary star to the primary). In their quiescent states, they are extremely faint, with a typical optical magnitude of V$\sim$20; in their outburst states the optical brightness rises by several magnitudes, corresponding to a one hundred-fold increase in the optical luminosity. The change in X-ray brightness is even more spectacular, increasing a million-fold at outburst. This increase in the bolometric luminosity is caused by accretion of the disc material onto the compact object. It can take a year or more for the system to fade back to its pre-outburst magnitude; it may remain at this level for a number of decades before undergoing another outburst.

During outburst, the light output from the disc renders the secondary star unobservable. As a result, the orbital parameters of the system cannot be determined until the system is nearing quiescence. However, even in quiescence, the disc luminosity in the optical can be a considerable fraction of the secondary star's output [e.g. McClintock & Remillard (1986)], making any determination much more problematical. As one approaches the longer wavelengths, however, this disc contamination decreases, usually to a negligible level in the infrared H and K bands [demonstrated for V404 Cyg by Shahbaz et al. (1996a)]. It is in these wavebands that one is best able to determine the orbital parameters of the system during its quiescent state.

The parameter of interest to us in our present program is the mass of the unseen component, namely that of the compact object. A measurement of the radial velocity amplitude and orbital period of the secondary star provides us with a value of the mass function. This represents a dynamical measurement of the lower limit to the mass of the compact object. If this lower limit is greater than the theoretical upper limit to the mass of a neutron star (~3.2M$_\odot$, Friedman & Isper 1987) then it represents evidence suggesting that the compact object may be a black hole.

A further constraint may be placed on the mass of the compact object by a study of the observed (so-called "ellipsoidal") flux variations from the secondary star during the quiescent state of the system. The luminosity of the secondary star remains constant over an orbital cycle but, because it has been distorted by the gravitational field of the compact object, the area of the star presented towards the observer varies with orbital phase; since the observed flux is proportional to the area presented, this causes the apparent variation in flux that is seen from the system during quiescence. For a star of given spectral type, the size of any ellipsoidal modulation depends on three quantities: the relative masses of the binary components, the orbital inclination of the system to the observer's line of sight, and the wavelength of the observation; the presence of disc-light affects the size of the *observed* modulation, but this is a non-ellipsoidal component.

2 GRO J0422+32

2.1 History

GRO J0422+32 was discovered by the *Compton GRO* satellite on 1992 August 4, and reached a maximum of ~ 3 Crab (in the 40-150 keV energy range) on August 8 (Paciesas et al. 1992; Harmon, Fishman & Paciesas 1992). The optical counterpart was identified with a $V \sim 13$ star (Castro-Tirado et al. 1993), representing an outburst of over nine magnitudes, the largest yet recorded in this class, with a recurrence time of >64 yrs (Shao 1992; Castro-Tirado et al. 1993). A rather unusual feature of this system was the occurrence of two lesser optical outbursts over one year after the primary X-ray outburst, never before observed in this class. They occurred in Aug and Dec 1993 (days 370 and 480 after the peak of the X-ray outburst), with a $\Delta V \sim 5$, each lasting a total of ~ 30 days; each outburst was also followed by a series of smaller amplitude outbursts, the so-called "after-events" (Chevalier & Ilovaisky 1995).

By the end of January 1994, GRO J0422+32 seemed to have levelled off to a quiescent magnitude of V=20.7 (Zhao et al. 1994a; Martin & Serra-Ricart 1994; Chevalier & Ilovaisky 1994; Bonnet-Bidaud & Mouchet 1995), but by September of the same year it had fallen again to V=22.4 (Zhao et al. 1994b), a level at which it seems to have remained, at least until day ~ 960 (after the peak of the X-ray outburst), the last published magnitude of the system (Garcia et al. 1996). However, a ~ 0.5 mag dip below this level is seen between days ~ 860-870, suggesting that there may still be some lingering activity - see fig. 1 of Garcia et al. (1996) for the composite light curve.

2.2 The orbital period

Various orbital periods have been put forward for this system, all close to 5.1 hr. Chevalier & Ilovaisky (1996) have shown that the period that fits both their extensive photometric data and the spectroscopic data of Filippenko et al. (1995) is $P_{orb} = 0.212140 \pm 0.000\,003$ d. We use the orbital phase zero of $T_0 = HJD\ 244\ 9661.4278 \pm 0.0012$, taken from the radial velocity study of the motion of the secondary star by Filippenko et al. (1995) but adjusted such that it is defined as the point of inferior conjunction of the late-type star (when the secondary star lies along the line of sight between the Earth and the compact object). The high accuracy in both of these figures has enabled us to reinterpret observations made by other observers at earlier epochs, *before* the true period and phasing were known. We discuss some of these observations below.

2.3 Optical spectra

The first indication of the presence of the secondary star from optical spectroscopy was in the Doppler tomograms of Casares et al. (1995a). Their data were taken ~16 months after the peak of the X-ray outburst, ~9 months before quiescence. The Balmer emission at low velocity was attributed to the irradiated inner face of the secondary star, with the slightly higher velocity He II λ4686 emission attributed to a hot-spot. Using the ephemeris given above to calculate the phasing of these features, we can confirm that their interpretation is correct. By modelling the tomograms under these assumptions they derive a value of the mass function f(M)~1.2M$_\odot$. Unambiguous detection of the secondary star had to wait until the spectroscopy of Orosz & Bailyn (1995), Casares et al. (1995b) and Filippenko et al. (1995), taken over two years after the peak of the X-ray outburst, which show TiO bands and other lines typical of an M2 V dwarf star.

2.4 Mass function

The quiescent optical spectroscopy of Orosz & Bailyn (1995) taken 1994 Nov 5-7 shows double-peaked Hα in emission. Modelling this with optically thin accretion discs, and by using an empirical relation between the projected velocity of the outer disc and the semi-amplitude radial velocity of the secondary star for other black hole X-ray novae, they derive a mass function of f(M)=0.9±0.4M$_\odot$. This is consistent with f(M)=0.85±0.30M$_\odot$ that Casares et al. (1995b) measure from a least-squares sine fit to their quiescent optical spectra of 1994 Dec 28, using the ephemeris calculated from their photometry data obtained on 1994 Nov 8 and Dec 22-29. Their spectral classification is M2±2 V. Optical spectra taken in 1994 Nov 8,9 and 1995 Jan 26,7 (also in quiescence) by Filippenko et al. (1995) show the secondary star to be close to M2 V, and yield a mass function of f(M)=1.21±0.06$M_\odot$ (1σ), consistent with the previous two values. Note that the estimate of f(M)~1.2$M_\odot$ (stated without error estimate) from the Doppler tomography of Casares et al. (1995a) is close to the value derived from the quiescent spectroscopy. This implies that Doppler tomography may indeed be used to estimate the system parameters during the outburst phase, long before the system has approached quiescence.

Table 1. Journal of observations of GRO J0422+32

Date (Dec. '94)	No. Useable Frames	Phase Covered	Mean Seeing (arcsec)
8th H	37	0.63 - 0.79	1.06
K	293	0.02 - 1.11	1.04
9th H	342	0.50 - 1.83	1.45
K	66	0.15 - 0.47	1.54

2.5 Extinction

From the diffuse interstellar feature at 5780Å Shrader et al. (1994) calculate the colour excess to be $E(B-V) = 0.2\pm0.1$. By fitting a power-law to the optical continuum, the same authors obtain a value of $E(B-V) = 0.23\pm0.02$. Both these values are consistent with each other, and with the value of $E(B-V) = 0.3\pm0.1$ from Callanan et al. (1995). The latter quantity was calculated from four interstellar lines (at 5890, 5778, 5780 and 5797Å). However, Shrader et al. (1994) also derive a value of $E(B-V) = 0.40 \pm 0.06$ from the UV (*IUE* data) 2170Å interstellar feature, clearly inconsistent with the earlier values. Interestingly, this value is consistent with the value of $E(B-V) = 0.40 \pm 0.07$ that Chevalier & Ilovaisky (1995) derive from the $B-V, V-I_c$ sequence that is defined by 12 stars surrounding GRO J0422+32. However, the latter method takes no account of the varying distance between the individual background stars, or of that between the background stars and GRO J0422+32. The colour excess also may vary between the UV and the infrared. Here, we take the colour excess to be $E(B-V) = 0.3 \pm 0.1$, which brackets all the measurements.

3 OBSERVATIONS

Data were collected over two nights in Dec 1994 from the InSb infrared array IRCAM-3, with a scale of 0.286 arcsecs per pixel, on the 3.8m United Kingdom Infrared Telescope (UKIRT) atop Mauna Kea, Hawaii. H (16500Å) and K (22000Å) band photometry of GRO J0422+32 were obtained, and a log of the observations is given in Table 1. Some frames on one of the nights were taken out-of-focus (due to a sudden temperature drop), and these were ignored in the analysis. Long periods of photometric conditions allowed the acquisition of some UKIRT standards; this enabled the H and K magnitudes and colour of the system to be determined.

R-band photometry was also taken over four nights in 1995 Jan 12-15 from the back-illuminated Loral 1200 x 800 CCD, with a scale of 0.5 arcsecs per pixel, on the Perkins 1.8m telescope (at the Lowell Observatory, Arizona) with the IFPS (Pogge et al. 1995) in direct mode. We obtained 8, 18, 15, and 14 measurements of J0422+32 on the nights of Jan 12, 13, 14, and 15 respectively, each with an integration time of 20 min. Sky conditions were clear and the seeing was typically 2.0-2.5 arcsec FWHM. The reduction of the R-band data utilised dome flats and the aperture photometry of the IRAF software; the 2σ detection limit of each 20 min frame is $R = 24.2$ mag.

The infrared H, K data were treated differently. The $H(K)$-band data frames were taken in groups of 3(4) co-adds of 15(10) seconds, and so each frame represents a 45(40) second exposure. Co-adds are used to optimise the signal-to-noise ratio of the fainter stars within a field without saturating the brighter ones. After each exposure, the telescope is moved by a small amount in RA and DEC. This causes the star of interest to fall on different parts of the array. The telescope motion is cyclic, and after one cycle the star of interest falls on (roughly) the same part of the array as in the first exposure. This exposure then marks the beginning of the next cycle, and the telescope repeats the same inter-exposure movements. The reason for observing in this fashion is that in each cycle of the telescope motion, any particular pixel will have been illuminated by the sky in at least one frame. This allows the sky to be used as a source of uniform illumination with which to remove the pixel-to-pixel sensitivity variations of the array. To do this, each frame is first of all dark subtracted, and then scaled, such that the mean value for every frame in the set is the same. For each frame in the set, a new frame is created by taking as the value for each pixel the median of the values it has amongst the remaining (scaled) frames from within that set; this new frame can then be used as a normal flat field image. This process is repeated for each frame from within the set (noteing that the frame to be flat fielded is not included in the median-stacking process).

GRO J0422+32 is roughly 12 degrees from the Galactic plane and is in a relatively uncrowded field, allowing simple aperture photometry to be used. The aperture photometry code has been described elsewhere (Shahbaz, Naylor & Charles 1994a) but it should be noted that the photometric accuracy of the routine depends on the size of the aperture used: too small an aperture and not enough of the stellar image is being sampled; too large an aperture and scatter from the sky background becomes important. For most of the data, an aperture size equal to four pixels ($\sim$1.14 arcsec) in radius was used. Poorer seeing on the 9th resulted in an aperture of eight pixels in radius being used for the K-band data of that night. Note however that the star five arcsec to the north-east of GRO J0422+32 still contributes less than one percent of the flux in this larger aperture.

Sky transparency variations between frames were removed by dividing the photometry of GRO J0422+32 by a weighted mean of the photometry of the two brightest, non-variable stars from within the same field (see Table 2), thus making the photometry relative. [See Shrader et al. (1994), Callanan et al. (1995) and Chevalier & Ilovaisky (1995) for finding charts.]

4 MODEL FITTING AND RESULTS

4.1 Magnitude and colour of GRO J0422+32

Absolute calibration of the HK data was made possible by the observation of standard stars on the night of 1994 December 8, with five frames in each of the H- and K- bands taken. By calculating a zero point magnitude from the standards, and by using the median values of the extinctions given in Krisciunas et al. (1987), the magnitudes of GRO J0422+32 and comparison stars were found, and are given in Table 2.

Using $E(B-V) = 0.3 \pm 0.1$ mags (see Section 2.5) the de-reddened colour of GRO J0422+32 is $H-K = 0.221 \pm$

Table 2. Mean magnitudes of GRO J0422+32 and comparison stars

Band	GRO J0422+32	Comparison	Standard-1	Standard-2
H	16.43 ± 0.03	16.20 ± 0.03	13.62 ± 0.02	15.09 ± 0.03
K	16.12 ± 0.04	16.31 ± 0.04	13.71 ± 0.02	15.14 ± 0.04

The comparison star is ∼5 arcsec north-east of J0422+32, while standards 1 and 2 are both ∼30 arcsec north-east and south-west of J0422+32 respectively (standard-2 is labelled as Star 4 in the Chevalier & Ilovaisky (1995) chart).

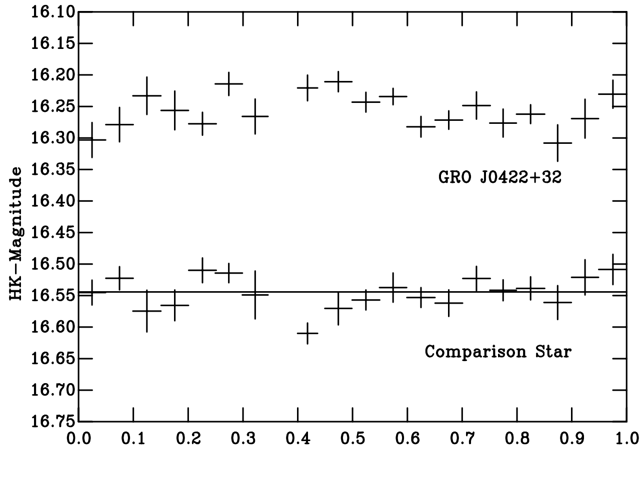

Figure 1. The combined infrared HK light curve for the LMXB transient system GRO J0422+32 at quiescence (1994 Dec 8,9th). The crosses are the individual data binned in phase bins of width 0.05, with the vertical error bars representing the sample error on the bin mean. The lowest curve is a comparison star (five arcsec north-east of GRO J0422+32) of similar magnitude to, and treated in exactly the same way as, GRO J0422+32. A constant of 0.25 mag has been added to the comparison star for clarity; the full line represents its mean.

0.092, consistent with an M2 dwarf secondary (Koornneef 1983), in line with the spectroscopic classification of other observers (e.g. Filippenko et al. 1995).

4.2 The infrared light curve

The data were then folded, using the ephemeris in Section 2.2, and binned into phase bins of width 0.05. Before the data were further processed, those points from within a given bin that were found to lie more than 3σ away from that bin's mean were discarded, and then the mean and sample standard error on the mean recalculated. This process removed 1 point each from the H- and K- band data sets. Considering the number of frames within the last two data sets (see Table 1), the number of points removed from each is not significant, indicating consistency within the data. The data were then converted from relative flux to apparent magnitude using the standard magnitudes given in Table 2. Note however that the errors quoted in this table are zero point errors and are not included in the calculation of the data point error bars; rather, they appear as an $\sim \pm 0.02$ magnitude uncertainty in the position of the magnitude scale (alternatively, in the mean magnitude of the system).

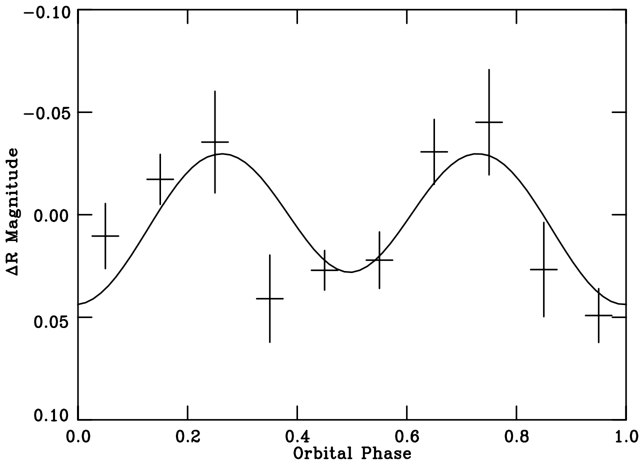

Figure 2. Our quiescent R-band light curve of 1995 Jan 12-15, binned into 10 phase bins; our best fit ellipsoidal model is also shown.

Neither the H- or K- band data sets showed any evidence of a "double-humped" ellipsoidal modulation, the only modulation being single humped. The H- and K- data were then combined (there is a less than 3 percent difference between the expected size of the ellipsoidal modulation in these bands), but weighted according to the mean error for each data set, in the hope that the underlying modulation might be revealed; it was not (see Figure 1). However, we can use the largest amplitude of an ellipsoidal modulation that could conceivably be hidden within the noise on the data to constrain the inclination of the system. For simplicity, we take the size of this amplitude to be the ~ 0.14 mag "hump" that the HK light curve displays, and use our model (to be described later) to generate the (i, q) range that is able to produce an ellipsoidal modulation with full amplitude less than or equal to this value, for input parameters appropriate to an M-star secondary. This shows that the inclination must be less than ~ 47 degrees, which translates into a lower mass limit of $\sim 4\mathrm{M}_{\odot}$.

4.3 The R-band light curve

Figure 2 shows our quiescent R-band data of 1995 Jan 12-15, folded on the ephemeris of Section 2.2 and binned into 10 phase bins. Each bin consists of at least 4 individual measurements with the point at phase 0.45 consisting of 8 measurements; the vertical error bars represent the standard deviation on each bins mean. This figure clearly shows a double-humped modulation with a full amplitude of ∼0.07 magnitudes. We have modelled this as an ellipsoidal modulation, with the figure showing our best fit plotted over this data.

Our model generates a light curve for a given mass ratio (q) and inclination (i) by assuming that each area element of the secondary star is a black body emitter and that the temperature varies over its surface according to Von Zeipel's (1924) gravity darkening law. The model light curve is then compared to that observed, using the χ^2 statistic to determine the best fit. The output of the model is a range of i for each of the input q values. From a knowledge of the value of the mass function

$$f(M) = M_1 \sin^3 i/(1+1/q)^2 \quad (1)$$

(where $q = M_1/M_2$, and M_1, M_2 are the masses of the black hole and secondary star, respectively) of the system, we can calculate M_1 for each q and its model-returned i value. Then, knowing M_1 for each q, we can trivially calculate M_2. This then allows us to plot M_1 against M_2. [For a detailed description of the model see Shahbaz, Naylor and Charles (1993)]. The mass function has been measured by Filippenko et al. (1995) to be $1.21 \pm 0.096 M_\odot$ (1.6σ).

The required parameters of the model are the wavelength (λ) of observation, effective temperature (T_{eff}) of the secondary star, the limb darkening coefficient (u) and gravity darkening exponent (β). Note that inclusion of the limb darkening coefficient results in the deepest minima occurring at phase 0.0 for low-inclinations (see e.g. Shahbaz 1994). The model was run with q ranging from 1 to 30, i ranging from 1 to 60 degrees, $\lambda = 7000$Å, $T_{eff} = 3500$ K, $u = 0.69$ (Al-Naimiy 1978), and with $\beta = 0.05$ (Sarna 1989); since the orbital period is now known with such high precision, phase zero was not left as a free parameter but held fixed. The best fit had a reduced chi-squared (χ^2_ν) of 2.0. This modelling constrains the inclination to be between $\sim$ 9-36 degrees, translating into a mass range of $\sim$ 7-400$M_\odot$. Clearly, this upper limit is well above the believed maximum mass that a black hole can have if from a stellar origin. Thus, these data provide no constraining information on the upper limit to the mass of the black hole. Physically, then, the only meaningful information that we can extract from this data is that the black hole mass must be larger than $\sim 7M_\odot$.

4.4 The R_c-band light curve

We have also modelled the Cousins R_c-band light curve of Chevalier & Ilovaisky (1996), taken on 1994 Nov 29, 30 and thus in quiescence. The data were modelled with $\lambda = 6000$Å and u=0.81, with the other parameters as before. This modelling also indicates an upper limit of $\sim$ 47 degrees for the inclination of the system. Figure 3 shows the data with the best fit model ellipsoidal modulation plotted; the best fit had a reduced chi-squared (χ^2_ν) of 3.93. This large χ^2_ν value is probably a result of our model not accounting for the high level of (perhaps variable) disc contamination that is expected to be present in this band.

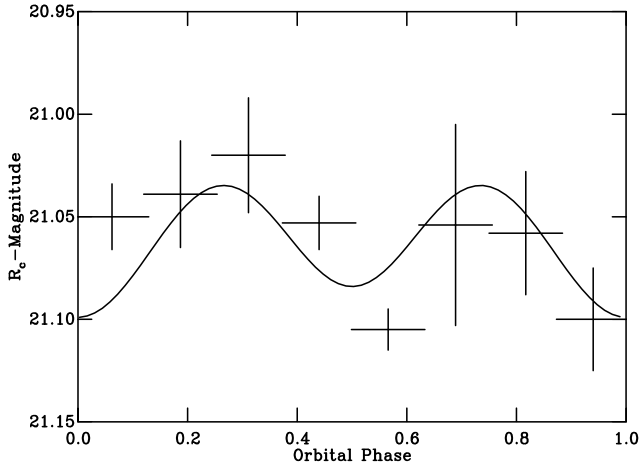

Figure 3. The quiescent R_c light curve of Chevalier & Ilovaisky (1996) taken 1994 Oct 29,30. The crosses are their binned data points; the full line is a plot of our best fit ellipsoidal model to their data.

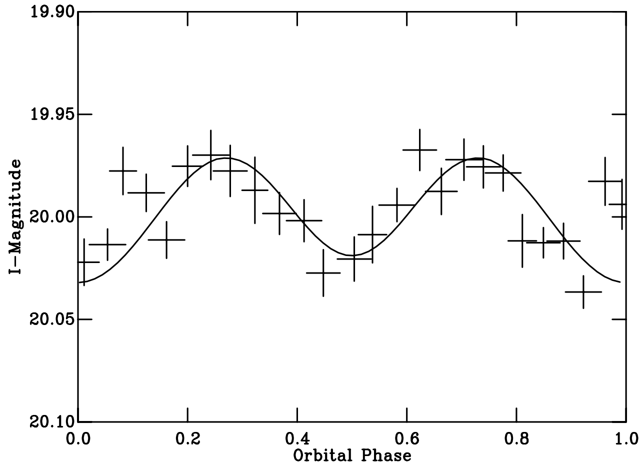

Figure 4. The quiescent I-band light curve of Orosz & Bailyn (1995) and Callanan et al. (1996) taken 1994 Oct 27, 28 and 1994 Dec 28, respectively. The crosses are their data points binned on 0.05 phase bins; the full line is a plot of our best fit ellipsoidal model to this data.

4.5 The I-band light curve

We also modelled the I-band data of Callanan et al. (1996) and of Orosz & Bailyn (1995), with both data sets read from Figure 1 (except exposure time, in text) of Callanan et al. (1996). These data were taken in 1994 Oct 27,28 and 1994 Dec 28, both during quiescence. The data were then folded using the ephemeris of Section 2.2, and binned into phase bins of width 0.05. The bin mean is the simple arithmetic mean, but note that the error on the bin mean was calculated using the error on each individual data point as a weighting factor. The binned data show a clear double-humped ellipsoidal modulation of full amplitude of $\sim$ 0.1 magnitudes. The data were modelled with $\lambda = 9000$Å and u=0.57, with the other parameters as before. Figure 4 shows the data with the best fit model ellipsoidal modulation plotted as a solid line; the best fit had a χ^2_ν=2.76. The inclination is constrained to lie between $\sim$ 10 and 26 degrees, translating into a mass range of $\sim$ 15-232$M_\odot$ for the mass of the (unseen) compact object. Following the argument of Section 4.3, this data thus only provides a lower limit of $\sim 15M_\odot$ to the mass of the black hole. Figure 5 shows the range of allowed inclinations for each modelled data set, and Figure 6 shows the limits on the masses of the binary components that these inclination limits impose. The regions delineated in each figure are the 90 percent confidence regions, calculated according to Lampton, Margon & Bowyer (1976) after the error bars had been scaled to give χ^2_ν=1, and taking due account of the number of free parameters in each case.

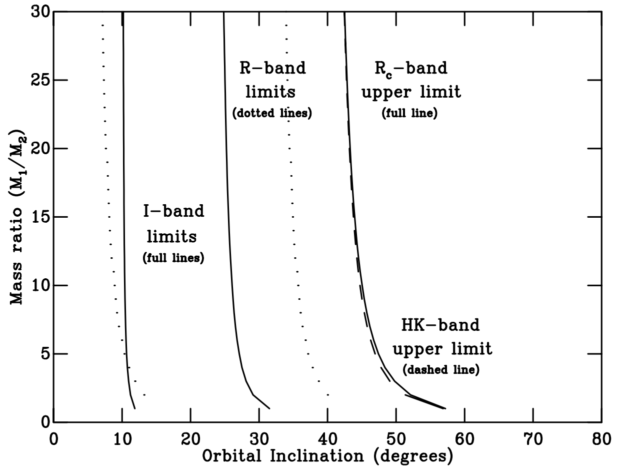

Figure 5. The mass-ratio–inclination information obtained from modelling the quiescent R, R_c, I and HK light curves of GRO J0422+32 as ellipsoidal modulations, with the 90 per cent confidence regions marked (upper limits only for the R_c and HK data).

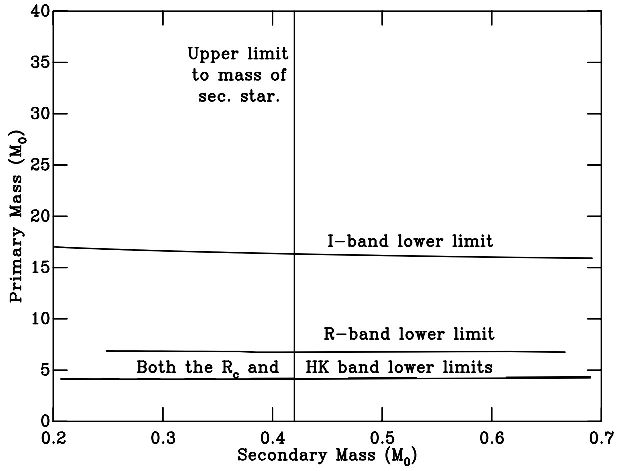

Figure 6. Plot showing mass of primary against mass of secondary, with the 90 per cent confidence region marked, obtained by modelling the R, R_c, I and HK band light curves of GRO J0422+32 as ellipsoidal modulations, and using the value of the mass function of Filippenko et al. (1995). The vertical line represents an upper mass limit to the secondary star of $0.42M_\odot$ (M2 V).

4.6 The case against a high inclination system

Kato, Mineshige and Hirata's (1995) outburst data of December 1992 and January 1993 show dips in some, but not all, of their light curves. Their *folded* light curve (their Fig. 7) shows a feature which they interpret to be a grazing eclipse of the disc by the secondary star, evidence of a system at high inclination. (Using the ephemeris given in Section 2.2, we calculate that the eclipse would actually be of the secondary star by the disc). This is clearly in contradiction with our suggestion that the system is at a *low* inclination.

If the system geometry is as Kato et al.'s folded light curve suggests, then this probably implies an inclination of ~80 degrees, and that the compact object is a neutron star, of mass (say) $M_1 \sim 2M_\odot$. The secondary is an M2 V, of mass $M_2 \sim 0.4M_\odot$. For a mass ratio of $q = 5$ ($q = M_1/M_2$) and an inclination of $i = 80$ degrees, the expected amplitude of the quiescent ellipsoidal modulation in the I-band is ~0.34 magnitudes, whereas the fitted amplitude to that observed in quiescence is only ~0.06 magnitudes. If the system really is at $q = 5, i = 80$ degrees, then the difference between the observed and expected amplitude of the ellipsoidal modulation implies that the disc is contributing an unusually large amount of light to the system in quiescence. This latter case implies that $f_{disc} \sim 4\,f_{2,max}$, where f_{disc}, $f_{2,max}$ represent the flux from the disc and the maximum flux observed from the secondary star, respectively. Thus, Kato et al.'s geometry implies that the disc is four times more luminous than the secondary star *in quiescence*.

However, Filippenko et al. (1995) estimate the quiescent contamination at $\lambda \sim 6300$Å to be between 30 - 60 percent, i.e. $f_{disc} \sim 0.3 - 0.6\,f_{system}$ (where $f_{system} = f_{disc} + f_2$), corresponding to $f_{disc} \sim 0.4 - 1.5\,f_2$. Our own photometric colours also suggest that the level of contamination is small, the colours being consistent with the spectroscopic classification of an M2 V star. Thus direct observational measurements are in contradiction with the values expected from the Kato et al. geometry, implying that the system is *not* at the high inclination that their interpretation suggests. We propose, then, that Kato et al.'s folded light curve, taken just five months after the peak of the X-ray outburst, is best explained as a single-humped modulation caused by the heated face of the secondary. The phasing is correct for such an interpretation if we use the ephemeris in Section 2.2. [The heated inner face of the secondary is also seen in the form of the Balmer emission at low velocity in the Doppler tomograms of Casares et al. (1995a).] The "grazing eclipse" feature observed is a result of an averaging of the random variations in the disc luminosity that occurred at that time, and is not a true eclipse feature.

Various authors have also pointed out that the double-peaked emission line profiles can be interpreted as arising from a disc viewed at high inclination, but no inclination-dependent modelling has yet been carried out. We note also that a double-peaked emission-line profile can occur for a system inclination as low as 15 degrees [see the models of Horne & Marsh (1986)], so double-peaks are, by themselves, not evidence of a high inclination. In addition, Orosz et al. (1994) have modelled the emission-line profiles of two other SXTs and find that they require optically-thick regions within the disc to reproduce the observed depth of the trough between the two peaks of the emission lines. However, the depth of these troughs are seen to vary both with orbital phase and with time, implying that the optically-thick regions migrate through the disc. This renders the depth of the trough inappropriate as an inclination diagnostic.

One may roughly determine the inclination of the system from the measured separation of the emission-line peaks, and from the assumption that the accretion disc fills 70 percent of the primary Roche-lobe. Assuming a black hole mass of $10M_\odot$ and a secondary of $0.42M_\odot$, the Keplerian velocity of the outer edge of the disc (v_d) may be calculated from $v_d = (GM_1/R_d)^{0.5}$, using Kepler's third law and Paczyński's (1971) formula for the size of the Roche lobe. Orosz & Bailyn (1995) measure, from the separation of the emission-line peaks, the projected velocity of the outer edge of the disc ($v_d \sin i$) to be 455±15kms^{-1}. The inclination (i) is then simply arcsin($v_d \sin i/v_d$); this gives i ∼23 degrees, consistent with our ellipsoidal model-estimated values. Note however that the assumption of Keplerian velocities at the outer edge of the disc may not hold (Orosz et al. 1994).

5 DISCUSSION

Disc contamination should decrease at longer wavelengths. It is thus surprising that the infrared HK-data show no sign of the double-humped ellipsoidal modulation that would be expected from this system in quiescence (see the references at the foot of Table 3 for examples of such curves). However such a modulation has been detected at shorter wavelengths, namely in the R, R_c and I bands. The amplitude of the modulation in these bands is consistent with its lack of detection in the infrared data, bearing in mind the sensitivity of the latter.

It is readily apparent that all of the data sets point toward GRO J0422+32 being a low inclination, black hole system. Although the I-band data constrain the system parameters well, they have been derived without negating the effect of a possible disc contribution to the flux. Taking as a reasonable example that $f_{disc} \sim 0.30\, f_{system}$, re-modeling the data with this level of contamination changes the results little. If there exists a 30 percent contamination level then our ellipsoidally derived inclination limits are 13-31 degrees, implying a black hole mass larger than ∼ 9 M$_\odot$.

The de-reddened $H-K$ colour of the system is 0.221 ± 0.092 magnitudes, consistent with the spectroscopic classification of an M0/M2 V star. This indicates that the disc contamination in the infrared is small. As already noted, Filippenko et al. (1995) measure the contamination at $\lambda \sim 6300$Å to be between 30 and 60 percent. Since the I-band lies between these two, a 30 percent level of contamination is not too unrealistic an estimate. Thus, our ellipsoidal modelling combined with this level of contamination predicts that the system is at low inclination, and contains a black hole of high mass.

This prediction is further strengthened by the following. A recent paper by King, Kolb and Burderi (1996) presents an equation which shows that for SXTs with binary periods $P_{orb} \lesssim$2 days, one can estimate the evolutionary status of the secondary star for a given compact object mass. This shows that, for transient behaviour, systems that contain a neutron star have secondaries that are more evolved than if the same compact object were a black hole. We show that their equation may be used in the opposite sense, to estimate the mass of the compact object from a separate estimate of the evolutionary status of the secondary star. If our ellipsoidal modelling is correct, one would expect both methods of mass determination to be in agreement; here, we show that they are.

The analysis of King et al. assumes that the X-ray binaries formed under the condition that their angular momentum loss time-scales are comparable to their nuclear evolution time-scales, implying that the secondary star had evolved off the main sequence before making the initial contact with its Roche-lobe surface. Evolution of the binary is then dominated by angular momentum losses (such as magnetic braking and the emission of gravitational radiation) and not on the nuclear evolution of the secondary star (now said to be "frozen in"). Evolutionary tracks (Pylyser & Savonije 1988a,b) show that these systems evolve towards shorter periods as the secondary (or donor) star loses mass to the accreting object, eventually becoming what we see as a short period X-ray binary. Assuming that the transient outburst is the result of a disc instability, it is then the rate of the mass transfer which determines whether the system becomes persistent or transient.

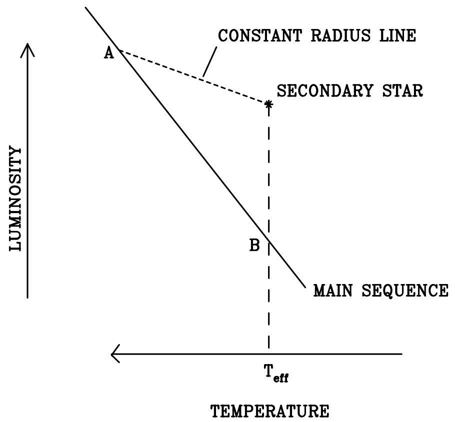

Figure 7. A schematic of the Hertzsprung-Russell diagram, showing a section of the lower main sequence and the position of an evolved secondary star. See the Discussion for the details.

In the disc instability model, the mass transfer rate must be below a critical level before outbursts can occur. King et al. show that the presence of X-ray irradiation lowers this critical level. This leads them to the following equation for the compact object mass (M_1) that all SXTs with $P_{orb} \lesssim 2$ days must satisfy [see King et al. (1996) for the detail of its derivation],

$$M_1 > \frac{M_{min}\hat{m}_2^{7/4} P_3^{1/4}}{(1 - h\hat{m}_2^2 P_3^{-2})^{3/4}}, \qquad (2)$$

where $M_{min} \approx 16 M_\odot$, and $h \approx 1.52$ (M_{min}, h are a combination of magnetic braking and gravitational radiation terms); P_3 is $P_{orb,hours}/3.0$, and $\hat{m}_2$ is $M_2/M_2(MS)$ where M_2 is the present mass of the secondary star, and $M_2(MS)$ is the mass of a main sequence star that would just fill the Roche lobe at that period. Although not evident from its form, for these values equation 2 is a monotonically increasing function of $\hat{m}_2$. Thus, knowing the value of $\hat{m}_2$ allows one to place a lower limit on the mass of the compact object.⋆

Although we cannot measure $\hat{m}_2$ directly, we can calculate a lower limit to it from the corresponding ratio of densities. We can state trivially that $\hat{\rho}_2 = \hat{m}_2$, where

⋆ Note, however, that the denominator in eq. 2 must be larger than zero, producing the constraint that $P(\mathrm{hrs}) > 3.70\hat{m}_2$, where P(hrs) is the orbital period in hours. Since the maximum value of $\hat{m}_2$ is 1.0 then the maximum value of the minimum period is 3.7 hrs. All of the systems listed in Table 3 are comfortably above this period.

Table 3. System parameters and derived masses of some Galactic soft X-ray transients

System	Mass Function	Ellipsoidal Mass Estimates ($M_\odot$)	P_{orb}	$\bar{\rho}_2$ (g cm^{-3})	Spectral Type	$\rho(\mathrm{MS}, T_{eff})$ (g cm^{-3})	$\hat{\rho}_2$	Minimum Mass ($M_\odot$)
[1]V404 Cyg	6.08±0.06	10 - 15	6.5d	–	K0 IV	–	–	–
[2]Nova Muscae	3.01±0.15	4 - 11	10.4h	1.02	K4 V	2.94	0.35	4
[3]GS2000+25	4.97±0.10	5 - 15	8.3h	1.60	K5 V	3.07	0.52	7
[4]A0620-00	3.17±0.09	5 - 17	7.8h	1.81	K6 V	3.09	0.59	9
[5]GRO J0422+32	1.21±0.06	>9	5.1h	4.23	M2 V	3.59	>1.00	>32
[6]Cen X-4	0.21±0.08	0.5 - 2.1	15.1h	0.48	K7 V	3.10	0.15	1
[7]Aql X-1	-	-	19.0h	0.3	K0	2.19	0.14	1
[8]Nova Vel 1993	-	-	6.86h	2.40	<K7	<3.10	>0.77	>14
[9]V821 Ara	-	-	14.83h	0.50	<K7(?)	<3.10	>0.16	>1
[10]BW Cir	-	-	15.6h	0.45	<K7(?)	<3.10	>0.15	>1

Data from references:- 1,2,4,6,8: Shahbaz et al. 1994b, 1997, 1994a, 1996b, 1993. 3,5: Beekman et al. 1996, this paper. 7: van Paradijs & McClintock 1995 9: van Paradijs 1995. 10: Martin 1996.
Notes. $\rho(\mathrm{MS}, T_{eff})$ is the mean density, from Gray (1992), of the secondary star inferred from its spectral type.
$\bar{\rho}_2$ is the mean density calculated from the formula $\bar{\rho}_2 \approx 110/P_{hrs}^2 \mathrm{gcm}^{-3}$ [e.g. King (1989)].
$\hat{\rho}_2$ is the lower limit to $\hat{m}_2$, which is used to calculate the minimum mass that a system must possess in order to be transient, from the formula of King et al. (1996). The minimum mass values quoted in the last column have been rounded up to the nearest integer, reflecting the uncertainties in both the spectral classification and in our knowledge of lower main-sequence densities, and the fact that we have used the $\hat{\rho}_2$ as an approximation to $\hat{m}_2$.
See the Discussion for details.

$\hat{\rho}_2 = \rho_2/\rho_2(\mathrm{MS})$. The numerator is a simple function of the orbital period and so makes it an attractive quantity to use. Obviously $\rho_2(\mathrm{MS})$ is unknown because we do not know R_{lobe}, the Roche lobe radius of the secondary star in the binary. However, we can estimate an upper limit to $\rho_2(\mathrm{MS})$ by the following.

Fig. 7 shows a schematic drawing of the HR-diagram. The secondary star has evolved off the main sequence, and is now in contact with its Roche lobe surface (see the evolutionary models of Pylyser & Savonije 1988a,b). Point A on this figure represents a main-sequence star with radius=R_{lobe}, and hence has a density of $\rho_2(\mathrm{MS})$. Point B represents a main sequence star of similar spectral type (or T_{eff}) to that of the secondary star in the binary. Since density increases as we go down the main sequence, star 'B' has a larger density than star 'A'. We define the density of star 'B' to be $\rho(\mathrm{MS}, T_{eff})$, and thus $\rho_2(\mathrm{MS}) < \rho_2(\mathrm{MS}, T_{eff})$. Then

$$\frac{\rho_2}{\rho(\mathrm{MS})} > \frac{\rho_2}{\rho(\mathrm{MS}, T_{eff})}. \tag{3}$$

Substituting the *RHS* of eq. 3 for $\hat{m}_2$ in eq. 2, we see that M_1 obtained this way is a lower limit to the minimum mass of the compact object. This analysis will only be incorrect if the secondary star evolves below the main sequence, at which time nuclear burning will be nearing its end.

To calculate $\hat{\rho}_2$ we use the following. For a Roche-lobe filling star, the average density ($\bar{\rho}_2$) is a simple function of the orbital period [e.g. King 1989]

$$\bar{\rho}_2 = \rho_2 \approx \frac{110}{P_{hrs}^2} \text{ g cm}^{-3}. \tag{4}$$

The density of an isolated lower main-sequence star depends on the theoretical mass–radius relationship used, and on the metallicity. Here, we use the relationship of Gray (1992).

With this information, we can thus compute a lower limit to the value of $\hat{m}_2$, and use equation 2 to calculate a lower limit to the minimum mass that the primary star must possess for the observed transient behaviour to occur. We have calculated this quantity for each of the soft X-ray transient systems listed in Table 3 (except V404 Cyg, whose orbital period is too long for this analysis). An estimate of each compact object's mass-range has already been obtained from an infrared study of their ellipsoidal brightness variations. It can be seen from the table that the two separate mass estimates are in close agreement, with the $\hat{\rho}_2$-estimated mass lying close to the minimum of the ellipsoidally-determined mass range. Note that, in all cases, the $\hat{\rho}_2$ mass-estimate is larger than the corresponding value of the mass function.

This analysis offers a new method of determining the nature of the compact object in the soft X-ray transients. As one can see from Table 2, it correctly distinguishes between neutron star (Cen X-4 and Aql X-1) and black hole primaries (entries 2 - 5 in the table). Since all that is required is the binary period and spectral classification of the secondary star, this method provides the spectroscopist with an immediate answer to the question of the nature of the compact object.

Note that using Allen's (1981) density values in the minimum mass calculation raises the individual mass estimates by $\sim$ 50 percent but still correctly distinguishes between black hole and neutron star primaries. Alternatively, using Popper's (1980) review values reduces the minimum mass estimates but, again, still generally distinguishes between black hole and neutron star primaries. Andersen's (1991) compilation shows quite clearly that there is an intrinsic spread, caused by main-sequence evolution, in stellar parameters such as mass and radius. These can only be uniquely determined if one knows the age and metallicity etc. of the star in question. Compilations of single star parameters are therefore an average over evolutionary age within the main-sequence band. However, even though the minimum mass is critically dependent on the mass-radius relationship used, use of such averages or of less modern estimates does not significantly affect the overall result. (Except, perhaps, for M-stars – see also Caillault & Patterson (1990), Henry & McCarthy (1993), Kirkpatrick et al. (1993), Popper (1993), Weis (1993), Reid, Hawley & Gizis (1995), and Tout et al. (1996) for recent work on the lower main-sequence.) That is, this method correctly identifies the nature of the compact object in the soft X-ray transient binaries.

For the system of interest to this paper (GRO J0422+32) $\hat{\rho}_2 > 1$, opposite to what one would expect. This could be indicating that the secondary star in GRO J0422+32 is the least evolved of the systems in Table 3. If we take $\hat{m}_2 \approx 1$ we see that the minimum mass must be larger than $\sim 32 M_{\odot}$, consistent with our earlier estimates. However, a more likely explanation for the fact that $\hat{\rho}_2 > 1$ is to be found in the uncertainties in the mass–radius relationships for M-type stars. Taking Allen's value, we get a minimum mass of $\sim 28 M_{\odot}$.

Two other possibilities exist: GRO J0422+32 may have been classified as earlier than it actually is, or the system may be so old as to have evolved below the main sequence. If either of these two cases prove correct, the effect will be to reduce the size of the minimum mass. Note, however, that the density fraction (and hence the minimum mass) seems to be proportional to the spectral type for the black-hole candidates listed in Table 3 (Nova Muscae, GS2000+25 and A0620-00). Although there are only three members in this group, it is perhaps indicating that, since GRO J0422+32 is of a much later spectral type, the density fraction should be larger than ~ 0.65, say, which translates into a minimum mass of $\sim 10 M_{\odot}$. Given all these uncertainties, the best we can say is that this method also indicates the presence of a black hole in GRO J0422+32, with a mass larger than $\sim 28 M_{\odot}$. Thus, an entirely different line of reasoning also predicts the presence of a massive black hole in this system.

6 CONCLUSIONS

We have shown that the orbital dips seen in the optical light curve of GRO J0422+32, as observed by Kato et al. (1995) five months after the peak of the X-ray outburst, are not consistent with an eclipse feature. A more likely explanation is that the so-called dips are random variations in the luminosity of the disc during this early period of its outburst phase. This highlights the danger involved in the interpretation of outburst data. In saying that, however, we point out that during the latter stages of outburst one may estimate the mass function of the system from Doppler tomography. This estimation depends on a correct interpretation of the tomograms and can lead to more than one estimate under differing assumptions. Again, this highlights the difficulty involved with outburst data.

Quiescent data are less problematical in their interpretation, and allow the system parameters to be determined more precisely. Ellipsoidal modelling of I-band data taken in quiescence, supported by quiescent R, R_c, H and K band data, show that the system has an inclination of between 10 and 26 degrees. Using the measured value of the mass function, this implies that GRO J0422+32 contains a black hole with a mass larger than ~15 $M_{\odot}$. These results have been calculated for the limiting case of zero flux contribution from the disc. However, even re-modelling the data with a 30 percent contamination level changes the result little: the inclination is constrained to lie between 13 and 31 degrees, implying that the black hole mass must be larger than ~9 $M_{\odot}$.

Using an equation discovered by King, Kolb and Burderi (1996) that describes the stability of the disc, we showed that it may be used to estimate a lower limit to the mass of the compact object in an SXT. The mass predicted by this method is larger than the corresponding mass function for each of the five systems tested, and lies within their ellipsoidally determined mass range. The method was also applied to three other systems with known orbital periods but of unknown spectral type, predicting a black hole in Nova Vel 1993, but allowing the possibility of a neutron star in both V821 Ara and BW Cir. Applying the method to GRO J0422+32, it indicates the presence of a black hole with a mass larger than $\sim 28 M_{\odot}$ (although uncertainties in the mass-radius relationships for M stars may affect this value).

We thus conclude that GRO J0422+32 is a system at low inclination that contains a high mass black hole. Our result is the lowest inclination and, consequently, the highest mass claim yet made for this system and definetly promotes GRO J0422+32 to the black hole-candidate class of soft X-ray transients. Indeed, it may be that GRO J0422+32 has the largest black hole mass of all the SXTs so far observed.

ACKNOWLEDGEMENTS

The United Kingdom Infrared Telescope is operated by the Royal Observatories on behalf of the UK Particle Physics and Astronomy Research Council; its data reduction was carried out on the Keele Starlink node using the ARK software. The Perkins 1.8m telescope is operated by the Ohio Wesleyan and Ohio State Universities at the Lowell Observatory; data reduction was performed at Ohio using the IRAF software. TN acknowledges the support of a PPARC Advanced Fellowship, and TS acknowledges the support of a PPARC Fellowship.

The lead author dedicates this paper to the memory of his good friend Paul Grant (1971-96), who died tragically in a motorcycle accident during the completion of this paper. His contribution to the educational charity A.S.T.R.A., the Association in Scotland to Research into Astronautics Ltd., will be sorely missed.

REFERENCES

Allen C.W., 1981, *Astrophysical Quantities*, 3rd edn, Athlone Press, London
Andersen J., 1991, Astron Astrophysics Rev, 3, 91
Al-Naimiy H.M., 1978, Ap&SS, 53, 181
Beekman G., Shahbaz T., Naylor T., Charles P.A., 1996, MNRAS, 281, L1
Bonnet-Bidaud J.M., Mouchet M., 1995, A&A, 293, L69
Bradt H.V.D., McClintock J.E., 1983, ARA&A, 21, 13
Cailault J.P., Patterson J., 1990, AJ, 100, 825
Callanan P.J., Garcia M.R., McClintock J.E., Zhao P., Remillard R.A., Bailyn C.D., Orosz J.A., Harmon B.A., Paciesas W.S., 1995, ApJ, 441, 786

Callanan P.J., Garcia M.R., McClintock J.E., Zhao P., 1996, ApJ, 461, 351
Casares H., Marsh T.R., Charles P.A., Martin A.C., Martin E.L., Harlaftis E.T., Pavlenko E.P., Wagner R.M., 1995a, MNRAS, 274, 565
Casares H., Martin A.C., Charles P.A., Martin E.L., Rebolo R., Harlaftis E.T., Castro-Tirado A.J., 1995b, MNRAS, 276, L35
Castro-Tirado A.J., Pavlenko E.P., Shlyapnikov A.A., Brandt S., Lund N., Ortiz J.L., 1993, A&A, 276, L37
Caillault J., Patterson J., 1990, AJ, 100, 825
Chevalier C., Ilovaisky S., 1994, IAU Circ. 5928
Chevalier C., Ilovaisky S., 1995, A&A, 297, 103
Chevalier C., Ilovaisky S., 1996, A&A, 312, 105
Cowley A., 1992, ARA&A, 30, 287
Filippenko A.V., Matheson T., Ho L.C., 1995, ApJ, 455, 614
Friedman J.L., Isper J.R., 1987, ApJ, 314, 594
Garcia M.R., Callanan P.J., McClintock J.E., Zhao P., 1996, ApJ, 460, 932
Gray D.F., 1992 *The Observation and Analysis of Stellar Photospheres*, 2nd ed., Cambridge University Press, p430
Harmon B.A., Fishman G.J., Paciesas W.S., 1992, IAU Circ. 5685
Henry T.J., McCarthy D.W., 1993, AJ, 106, 773
Horne K., Marsh T.R., 1986, MNRAS, 218, 761
Kato T., Mineshige S., Hirata R., 1995, PASJ, 47, 31
King A.R., 1989 *Classical Novae*, eds Bode M.F. & Evans A., p17-39
King A.R., Kolb U., Burderi L., 1996 ApJ 464 L127
Kirkpatrick J.D., Kelly D.M., Rieke G.H., Liebert J., Allard F., Wehrse R., 1993, ApJ, 402, 643
Koornneef J., 1983, A&A, 128, 84
Krisciunas K. et al. 1987, PASP, 99, 887
Lampton M., Margon B., Bowyer S., 1976, ApJ, 208, 177
Martin A., 1996, PhD thesis, Oxford University
Martin E., Serra-Ricart M., 1994, IAU Circ. 5967
McClintock J.E., Remillard R.A., 1986, ApJ, 308, 110
Orosz J.A., Bailyn C.D., Remillard R.A., McClintock J.E., Foltz C.B., 1994, ApJ, 436, 848
Orosz J.A., Bailyn C.D., 1995, ApJ, 446, L59
Paciesas W.S., Briggs M.S., Harmon B.A., Wilson R.B., 1992, IAU Circ. 5580
Paczyński B., 1971, ARA&A, 9, 183
Pogge R.W., Atwood B., Byard P.L., O'Brien T.P., Peterson B.M., Lame N.J., Baldwin J.A., 1995, PASP, 107, 1266
Popper D.M., 1980, ARA&A, 18, 115
Popper D.M., 1993, ApJ, 404, L67
Pylyser E., Savonije G.J., 1988a, A&A, 191, 57
Pylyser E., Savonije G.J., 1988b, A&A, 208, 52
Reid I.N., Hawley S.L., Gizis J.E., 1995, AJ, 110, 1838
Sarna M.J., 1989, A&A, 224, 98
Shahbaz T., Naylor T., Charles P.A., 1993, MNRAS, 265, 655
Shahbaz T., Naylor T., Charles P.A., 1994a, MNRAS, 268, 756
Shahbaz T., Ringwald F.A., Bunn J.C., Naylor T., Charles P.A., Casares J., 1994b, MNRAS, 271, L10
Shahbaz T., PhD thesis, Keele University
Shahbaz T., Bandyopadhyay R., Charles P.A., Naylor T., 1996a, MNRAS, 282, 977
Shahbaz T., van der Hooft F., Charles P.A., Casares J., van Paradijs J., 1996b, MNRAS, 282, L47
Shahbaz T., Naylor T., Charles P.A., 1997, MNRAS, accepted
Shao C.Y., 1992, IAU Circ. 5606
Shrader C.R., Wagner R.M., Hjellming R.M., Han X.H., Starrfield S.G., 1994, ApJ, 434, 698
Tanaka Y., Lewin W.H.G., 1995, in X-Ray Binaries, ed. W.H.G. Lewin, J van Paradijs & E.P.J. van den Heuvel, (CUP), 126
Tout C.A., Pols O.R., Eggleton P.P., Han Z., 1996, MNRAS, 281, 257
van der Klis M., 1989, ARA&A, 27, 517
van Paradijs J., McClintock J.E., 1995, in X-Ray Binaries, ed. W.H.G. Lewin, J van Paradijs & E.P.J. van den Heuvel, (CUP), 58
van Paradijs J., 1995, in X-Ray Binaries, ed. W.H.G. Lewin, J van Paradijs & E.P.J. van den Heuvel, (CUP), 536
Verbunt F., 1993, ARA&A, 31, 93
Von Zeipel H., 1924, MNRAS, 84, 665
Weis E.W., 1993, AJ, 105, 1962
Zhao P., et al. 1994a, IAU Circ 5929
Zhao P., et al. 1994b, IAU Circ 6072